大韓獸醫學會誌 (2015) 第 55 卷 第 1 號
Korean J Vet Res(2015) 55(1) : 57~60
http://dx.doi.org/10.14405/kjvr.2015.55.1.57

<Short Communication>

Distribution and accumulation of ^{177}Lu-labeled thermally cross-linked superparamagnetic iron oxide nanoparticles in the tissues of ICR mice

Jin Joo Hue[1,†], Hu-Jang Lee[2,†], Sang Yoon Nam[1], Jong-Soo Kim[1], Beom Jun Lee[1,*], Young Won Yun[1,*]

[1]*College of Veterinary Medicine and Research Institute of Veterinary Medicine, Chungbuk National University, Cheongju 361-763, Korea*
[2]*College of Veterinary Medicine and Institute of Life Science, Gyeongsang National University, Jinju 600-701, Korea*

(Received: November 10, 2014; Revised: December 11, 2014; Accepted: December 29, 2014)

Abstract : To investigate kinetics of free ^{177}Lu and ^{177}Lu-labeled thermally cross-linked superparamagnetic iron oxide nanoparticles (TCL-SPION), suspensions were intravenously injected into the tail vein of mice at a dose of 5 μCi/mouse or 15 mg/kg body weight, respectively. Free ^{177}Lu radioactivity levels were highest in kidney followed by liver and lung 1 day post-injection. ^{177}Lu-labeled TCL-SPION radioactivity in liver and spleen was significantly higher compared to that of other organs throughout the experimental period ($p < 0.05$). Radioactivity in blood, brain, and epididymis rapidly declined until 28 days. Based on these results, TCL-SPION could be a safe carrier of therapeutics.

Keywords : accumulation, biodistribution, ^{177}Lu, nanotoxicity, TCL-SPION

Many previous studies were performed to investigate the potential of magnetic nanoparticles as the drug-delivery vehicle [1, 7]. This characteristic makes them attractive for many applications, ranging from contrast enhancing agents for MRI to drug-delivery systems [5].

Research on the superparamagnetic iron oxide nanoparticles (SPION) has already demonstrated that these nanoparticles have the potential becoming an important tool for enhancing magnetic resonance contrast [2, 8]. All of these biomedical applications require that the nanoparticles have high magnetization values, a size smaller than 100 nm, and a narrow particle size distribution [5]. The magnetic nanoparticles have many advantages including thermal therapy, guiding to the target site, and relatively non-toxic [15]. These applications also need peculiar surface coating of the magnetic particles, which has to be nontoxic and biocompatible and must allow for a targetable delivery with particle localization in a specific area. Such magnetic nanoparticles can bind to drugs, proteins, enzymes, antibodies, or nucleotides and can be directed to an organ, tissue, or tumor using an external magnetic-field [3]. More importantly, iron oxide nanoparticles have a long blood retention time, biodegradability and low toxicity [6, 7]. Recently, anti-biofouling polymer-coated TCL-SPION was reported as a novel diagnostic probe for *in vivo* cancer imaging [9, 10].

Lutetium 177 (^{177}Lu), a, γ and β emitter radionuclide, is presently considered useful for a potential bone pain palliation agent owing to its suitable nuclear decay characteristics [$T_{1/2}$ = 6.73 days, $E_{\beta(max)}$ = 497 keV, E_{γ} = 113 keV (6.4%) and 208 keV (11%)] and the feasibility of large-scale production with adequate specific activity using moderate flux research reactors [3]. We investigated the distribution and accumulation of ^{177}Lu-labeled TCL-SPION and the *in vivo* kinetics of ^{177}Lu-labeled TCL-SPION on tissues of mice.

^{177}Lu (β = 495 keV, γ = 113 and 208 keV, $t_{1/2}$ = 6.7 days) purchased from Nuclear Research and Consultancy Group (Netherland). ^{177}Lu-labeled TCL-SPION (stability = 98% efficiency, period of efficiency = 21 days) was obtained from the Gwangju Institute of Science and Technology (Gwangju, Korea). SEM and TEM analysis of TCL-SPION were shown in Fig. 1. All other chemicals and reagents required for experiments were of analytical grade, and purchased from Sigma-Aldrich Chemical. (USA).

Sixty 5-week old male ICR mice were purchased from Koatec (Korea) at 21.3 ± 1.7 g in mass. Upon arrival, the mice were housed in a temperature- and humidity-controlled environment with a reversed 12/12 h light/dark cycle and free access to food and water. Animal experiments were performed in accordance with standard operation procedures of laboratory animals that were approved by the Institutional Animal Care and Use Committee of Chungbuk National University (approval no. CBNUR-284-27).

*Corresponding authors
Tel: +82-43-261-2597, Fax: +82-43-267-2595
E-mails: beomjun@cbu.ac.kr (Lee BJ), ywyun@cbu.ac.kr (Yun YW)
†The first two authors equally contributed to this work.

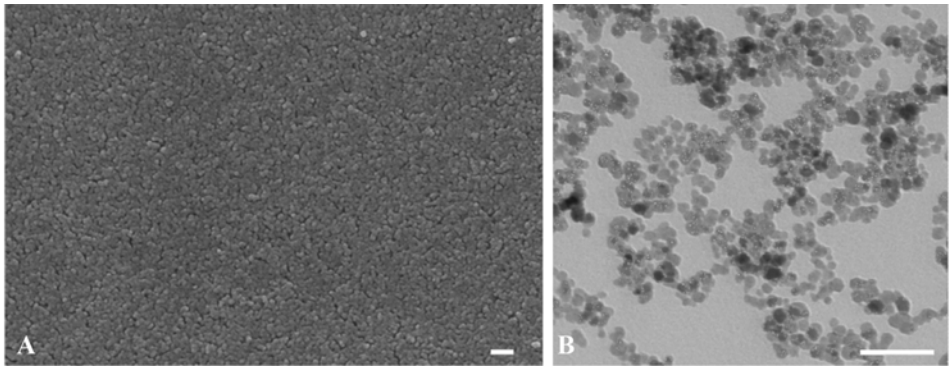

Fig. 1. (A) SEM analysis of thermally cross-linked superparamagnetic iron oxide nanoparticles (TCL-SPION). Nanoparticles had a smooth morphology. (B) TEM analysis of TCL-SPION. A: ×50,000, B: ×10,000. Scale bars = 100 nm (A), 50 nm (B).

After 1 week of acclimation, 50 μL of ^{177}Lu-labeled TCL-SPION (15 mg/kg body weight, n = 55) and free ^{177}Lu suspensions (5 μCi/mouse, n = 5) were intravenously injected in the tail vein of mice, respectively. At 1 day post-treatment, five mice injected with free ^{177}Lu suspensions were sacrificed and collected the blood and various organs (liver, kidney, spleen, heart, lung, stomach, small intestine and large intestine). At 0.25, 0.5, 1, 2, 4 h, 1, 3, 7, 14, 21 and 28-day post-injection, five mice injected with ^{177}Lu-labeled TCL-SPION were sacrificed by withdrawing blood from the heart under diethyl ether anesthesia. The various organs (liver, kidney, spleen, heart, small intestine, large intestine, lung, stomach, thymus, testis, epididymis, lymph node, brain) of each animal were also collected at 0.5, 2 h, 1, 7, 14, 21 and 28-day post-injection. The radioactivity in blood and organs was measured using a gamma counter (PerkinElmer, USA). Statistical analyses were carried out using a one-way analysis of variance (ANOVA) and Student's *t*-test. All data were expressed as the mean ± SD. p values < 0.05 were considered to be statistically significant.

Results of the analytical free ^{177}Lu radioactivity in blood and various organs of mice at one day-after treatment were shown in Fig. 1. In the average of free ^{177}Lu radioactivity, the kidney (2.62 ± 1.14%) was first, followed by the liver (2.02 ± 0.2%) and the lung (1.11 ± 0.56%), and the blood (0.19 ± 0.06%) was lowest. Due to partial reabsorption of radiolabelled peptides after glomerular filtration, the retention of free ^{177}Lu radioactivity in the radiosensitive kidney is substantial [11]. On the other hand, Persson *et al*. [12] reported that the mean of free ^{177}Lu radioactivity in the blood was the highest, followed by the kidney at one day post-injection of ^{177}Lu-labeled pertuzumab into BALB/c mice with the tumor. This result may be caused by the different of species and dosage of treatment. Fig. 2 shows the change of ^{177}Lu-labeled TCL-SPION level in the blood of mice during 28-day post-injection. At 0.25 h, ^{177}Lu-labeled TCL-SPION radioactivity in blood was 3.571 ± 0.679% injected dose (ID)/g and slowly declined in a time-dependent manner. Table 1 represents the biodistribution of ^{177}Lu-labeled TCL-SPION in blood and various organs of mice during 28-day post-injection. ^{177}Lu-labeled TCL-SPION radioactivity of liver and spleen was significantly different compared to that of blood and other organs throughout the experimental period ($p < 0.05$). The highest ^{177}Lu-labeled TCL-SPION radioactivity in liver and spleen was 36.121 ± 8.239% ID/g at one day post-injection and 15.615 ± 2.225% ID/g at 0.5 h post-injection, respectively, and that in kidney, and small and large intestine was observed at 2 h. At 0.5 h post-injection, other organs showed the highest ^{177}Lu-labeled TCL-SPION radioactivity.

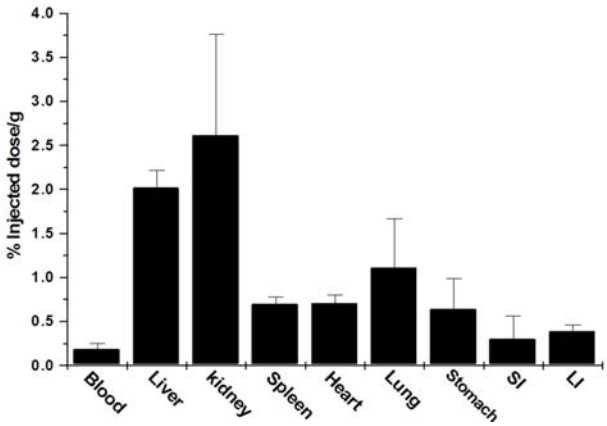

Fig. 2. Biodistribution of free ^{177}Lu activation in blood and various organs of mice at 1 day after treatment of free ^{177}Lu suspensions at a dose of 5 μCi/mouse. The bars were expressed as means ± SD. SI: small intestine, LI: large intestine.

In present study, ^{177}Lu-labeled TCL-SPION was immediately entered into the blood and rapidly eliminated during 0.25 h to one-day post-injection and then slowly eliminated thereafter (Fig. 3). This result suggests that the absorbed ^{177}Lu-labeled TCL-SPION was distributed from systemic circulation into the intracellular tissues. In the previous study, ferumoxides cleared very rapidly from plasma (elimination half-life of 6 min in rats) by uptaking of macrophages of the reticulo-endothelial system (mainly Kupffer cells in liver and spleen) [14]. Radioactivity of ^{77}Lu-labeled TCL-SPION in liver and spleen was higher than that in other organs during

Table 1. Biodistribution of ^{177}Lu-labeled TCL-SPION during 28 days in blood and various organs of mice intravenously injected with a single dose of 15 mg/kg body weight

Tissue	Time after treatment (% ID/g)						
	0.5 h	2 h	1 d	7 d	14 d	21 d	28 d
Blood	2.296 ± 0.292^{e}	1.234 ± 0.445^{de}	0.044 ± 0.019^{b}	0.015 ± 0.019^{ab}	0.010 ± 0.028^{ab}	< 0.001	< 0.001
Brain	0.037 ± 0.030^{a}	0.018 ± 0.005^{a}	0.009 ± 0.005^{a}	0.004 ± 0.002^{a}	0.002 ± 0.001^{a}	0.002 ± 0.001^{a}	< 0.001
Thymus	0.564 ± 0.167^{c}	0.404 ± 0.141^{bc}	0.203 ± 0.066^{d}	0.200 ± 0.49^{ef}	0.053 ± 0.029^{b}	0.216 ± 0.070^{cd}	0.115 ± 0.041^{bc}
Lymph node	0.595 ± 0.090^{c}	0.456 ± 0.112^{bc}	0.155 ± 0.045^{cd}	0.142 ± 0.040^{de}	0.160 ± 0.056^{de}	0.176 ± 0.067^{c}	0.181 ± 0.052^{c}
Heart	0.607 ± 0.143^{c}	0.491 ± 0.106^{bc}	0.177 ± 0.040^{d}	0.129 ± 0.030^{de}	0.108 ± 0.030^{cd}	0.149 ± 0.057^{c}	0.087 ± 0.035^{ab}
Lung	1.043 ± 0.186^{d}	0.893 ± 0.109^{d}	0.473 ± 0.180^{e}	0.237 ± 0.006^{f}	0.206 ± 0.055^{e}	0.173 ± 0.048^{c}	0.461 ± 0.178^{d}
Liver	31.283 ± 1.087^{g}	35.549 ± 2.093^{g}	36.121 ± 8.240^{h}	33.540 ± 2.740^{i}	24.521 ± 3.867^{h}	21.507 ± 1.648^{f}	15.147 ± 3.518^{f}
Spleen	15.615 ± 2.225^{f}	13.033 ± 1.280^{f}	14.622 ± 1.363^{g}	11.446 ± 1.320^{h}	9.269 ± 1.320^{g}	9.237 ± 1.350^{e}	9.094 ± 0.739^{e}
Kidney	1.189 ± 0.310^{d}	1.702 ± 0.334^{e}	1.066 ± 0.291^{f}	0.531 ± 0.076^{g}	0.525 ± 0.133^{f}	0.335 ± 0.063^{d}	0.365 ± 0.108^{d}
Stomach	1.286 ± 0.690^{c}	0.914 ± 0.452^{cde}	0.187 ± 0.057^{d}	0.160 ± 0.010^{e}	0.158 ± 0.010^{e}	0.132 ± 0.068^{c}	0.044 ± 0.010^{a}
Small intestine	0.347 ± 0.184^{bc}	0.487 ± 0.130^{b}	0.175 ± 0.068^{cd}	0.080 ± 0.028^{cd}	0.054 ± 0.033^{bc}	0.020 ± 0.023^{b}	0.073 ± 0.035^{ab}
Large intestine	0.327 ± 0.078^{b}	1.055 ± 0.295^{de}	0.142 ± 0.015^{d}	0.047 ± 0.022^{bc}	0.042 ± 0.027^{b}	0.027 ± 0.013^{b}	0.079 ± 0.010^{b}
Testis	0.311 ± 0.092^{b}	0.291 ± 0.089^{b}	0.065 ± 0.023^{bc}	0.053 ± 0.007^{c}	0.047 ± 0.030^{b}	0.049 ± 0.014^{b}	0.051 ± 0.016^{a}
Epididymis	0.661 ± 0.130^{c}	0.511 ± 0.167^{bc}	0.101 ± 0.021^{c}	0.081 ± 0.023^{cd}	0.003 ± 0.001^{a}	< 0.001	< 0.001

Means with the different letter in the same column are significantly different ($p < 0.05$).

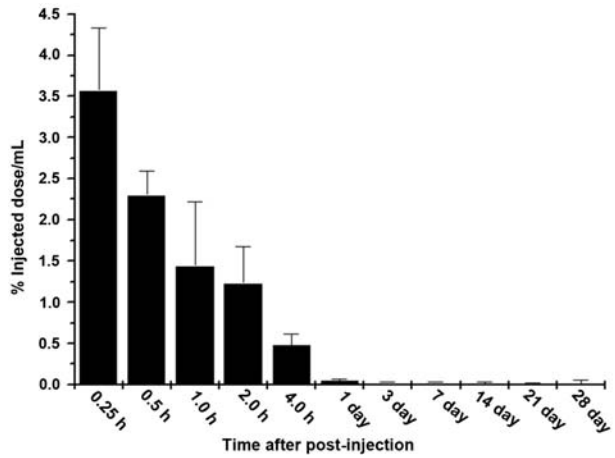

Fig. 3. Biodistribution of ^{177}Lu-labeled TCL-SPION during 28 days in the blood of ICR mice intravenously injected with single dose of TCL-SPION 15 mg/kg TCL. The bars were expressed as means ± SD.

experimental periods. Data were expressed as 15.1% ID/g in the liver and 9.1% ID/g in the spleen at 28 days. The iron contained in ferumoxtran-10 was incorporated into the body's iron store and was progressively found in hemoglobin [2]. A biodistribution study of MnMEIO-Herceptin conjugates labeled with radioactive ^{111}In using γ-counter analysis showed that in addition to being distributed within the tumor (3.4% injected dose ID/g), nanoparticles were also found on the liver (12.8% ID/g), spleen (8.7% ID/g) and muscle (1.0% ID/g) [8]. After intravenous injection, most SPIO nanoparticles were accumulated in the Kupffer cells in the liver and in the reticulo-endothelial system in the spleen [4]. Biodistribution of SPIO (AMI-25) measured by ^{59}Fe and relaxation time studies is consistent with a model of initial vascular distribution of the agent and specific uptake in reticulo-endothelial cells. These results from both techniques indicate similar initial distribution of intravenous administered AMI-25, with 85-95% uptake in the reticulo-endothelial system [14]. In other studies, after SPIO injection approximately 1 day, increases in T_2 and T_1 values of the precontrast baseline represent the dissolution of the crystalline form necessary for super-paramagnetic behavior. Interestingly, spleen displays a second peak of radioactivity after 60 days and clinical observation of reversal of liver and spleen signal intensity strengthened experimental evidence and suggested similar metabolism of iron oxide in humans [13]. These results were similar with the results from our study. In conclusion, the TCL-SPION was mainly accumulated in the liver and can be used for iron pool from the body iron stores.

Acknowledgments

This work was supported by the research grant of Chungbuk National University in 2012.

References

1. **Alexiou C, Schmid RJ, Jurgons R, Kremer M, Wanner G, Bergemann C, Huenges E, Nawroth T, Arnold W, Parak FG.** Targeting cancer cells: magnetic nanoparticles as drug carriers. Eur Biophys J 2006, **35**, 446-450.
2. **Bourrinet P, Bengele HH, Bonnemain B, Dencausse A, Idee JM, Jacobs PM, Lewis JM.** Preclinical Safety and pharmacokinetic profile of ferumoxtran-10, an ultrasmall superparamagnetic iron oxide magnetic resonance contrast

agent. Invest Radiol 2006, **41**, 313-324.
3. **Chastellain M, Petri A, Gupta A, Rao KV, Hofmann H.** Super paramagnetic silica-iron oxide nanocomposites for application in hyperthermia. Adv Eng Mater 2004, **6**, 235-241.
4. **Ferrucci JT, Stark DD.** Iron oxide-enhanced MR imaging of the liver and spleen: review of the first 5 years. AJR Am J Roentgenol 1990, **155**, 943-950.
5. **Gupta AK, Gupta M.** Synthesis and surface engineering of iron oxide nanoparticles for biomedical applications. Biomaterials 2005, **26**, 3995-4021.
6. **Harisinghani MG, Barentsz J, Hahn PF, Deserno WM, Tabatabaei S, van de Kaa CH, de la Rosette J, Weissleder R.** Noninvasive detection of clinically occult lymph-node metastases in prostate cancer. N Engl J Med 2003, **348**, 2491-2499.
7. **Jain TK, Morales MA, Sahoo SK, Leslie-Pelecky DL, Labhasetwar V.** Iron oxide nanoparticles for sustained delivery of anticancer agents. Mol Pharm 2005, **2**, 194-205.
8. **Lee JH, Huh YM, Jun YW, Seo JW, Jang JT, Song HT, Kim S, Cho EJ, Yoon HG, Suh JS, Cheon J.** Artificially engineered magnetic nanoparticles for ultra-sensitive molecular imaging. Nat Med 2007, **13**, 95-99.
9. **Lee H, Lee E, Kim DK, Jang NK, Jeong YY, Jon S.** Antibiofouling polymer-coated superparamagnetic iron oxide nanoparticles as potential magnetic resonance contrast agents for in vivo cancer imaging. J Am Chem Soc 2006, **128**, 7383-7389.
10. **Lee H, Yu MK, Park S, Moon S, Min JJ, Jeong YY, Kang HW, Jon S.** Thermally cross-linked superparamagnetic iron oxide nanoparticles: synthesis and application as a dual imaging probe for cancer in vivo. J Am Chem Soc 2007, **129**, 12739-12745.
11. **Melis M, Krenning EP, Bernard BF, Barone R, Visser TJ, de Jong M.** Localisation and mechanism of renal retention of radiolabelled somatostatin analogues. Eur J Nucl Med Mol Imaging 2005, **32**, 1136-1143.
12. **Persson M, Gedda L, Lundqvist H, Tolmachev V, Nordgren H, Malmström PU, Carlsson J.** [^{177}Lu]Pertuzumab: experimental therapy of HER-2-expressing xenografts. Cancer Res 2007, **67**, 326-331.
13. **Weissleder R, Bogdanov A, Neuwelt EA, Papisov M.** Long-circulating iron oxides for MR imaging. Adv Drug Deliv Rev 1995, **16**, 321-334.
14. **Weissleder R, Stark DD, Engelstad BL, Bacon BR, Compton CC, White DL, Jacobs P, Lewis J.** Superparamagnatic iron oxide: pharmacokinetics and toxicity. AJR Am J Roentgenol 1989, **152**, 167-173.
15. **Yu MK, Jeong YY, Park J, Park S, Kim JW, Min JJ, Kim K, Jon S.** Drug-loaded superparamagnetic iron oxide nanoparticles for combined cancer imaging and therapy in vivo. Angew Chem Int Ed Engl 2008, **47**, 5362-5365.